Hindawi
Advances in Mathematical Physics
Volume 2022, Article ID 7096486, 19 pages
https://doi.org/10.1155/2022/7096486

Research Article

New Solitons and Multishock Wave Structures for the Conformable Space Fractional Burger and Time Fractional Sharma-Tasso-Olver Models

Selina Akter,[1,2] Harun-Or-Roshid,[1] and N. F. M. Noor[3]

[1]*Department of Mathematics, Pabna University of Science and Technology, Pabna-6600, Bangladesh*
[2]*Department of Applied Mathematics, Gono Bishwabidyalay, Savar, Dhaka, Bangladesh*
[3]*Institute of Mathematical Sciences, Faculty of Science, Universiti Malaya, 50603 Kuala Lumpur, Malaysia*

Correspondence should be addressed to Harun-Or-Roshid; harunorroshidmd@gmail.com

Received 6 February 2022; Accepted 28 March 2022; Published 23 May 2022

Academic Editor: Mohammad Mirzazadeh

This present paper studies the conformable space fractional Burgers, and the time fractional Sharma-Tasso-Olver models; both are highly important for nonlinear diffusive waves in fluid dynamics, sound waves in a viscous medium, and flow in field soils, as well as in gas and plasma dynamics. To retrieve explicit solutions of the fractional differential models, we propose an integral scheme, namely, Modified Kudryashov method. We obtain periodic, solitary, mixed periodic-soliton, and polynomial solutions through the approach. In particular, we exhibit topological kink-dark bell wave, topological kink, singular kink, bright bell, peakon solitons, and periodic shape waves to apply suitable values on parameters for both distinct models. The impact of fractionality on the wave shape and its deformation is analyzed and discussed graphically. We also investigate multishock wave's solutions of both models and analyzed the effect of each existing parameters involved in the obtained solutions. To visualize the real characters of the solitary solutions, the graphical elucidation in 3D and 2D profiles are plotted. In computational effort and realization, it is emphasized that the proposed scheme is friendly useful, highly effective, and a powerful mathematical tool to extract exact solitary wave solutions for the differential models, as well as fractional differential models.

1. Introduction

Many natural phenomena in the fields of engineering; ocean engineering, fluid flows, mathematical biology, signal processing, optical communications systems, and electromagnetic theories are modeled in terms of fractional derivatives [1–11]. They have attracted high curiosities among the researchers owing to their occurrences in the modeling of complex physical phenomena. Therefore, solitary wave solutions for the relevant nonlinear problems are fundamental issues. A variety of powerful procedures have been explored to evaluate the solitary solutions of the various differential models with and without fractional derivatives in literature, such as Weierstrass elliptic function method [2], Laplace perturbation method [3], extended sinh-Gordon equation expansion method [4, 5], Darboux transformation [6], modified residual power series method [7], Bernoulli polynomial approaches [8], exp-expansion method [9], Adomian decomposition method [10], homotopy perturbation method [11], generalized Kudryashov method [12–14], (G'/G)-expansion method [15], and Hirota bilinear methods [16–20].

Nowadays, numerous efforts have been invested in execution of the above methods to derive exact soliton solutions for nonlinear differential models with space-time fractional. Moreover, fractional differential models have apparent huge devotion due to proper explanation of many nonlinear events [21, 22]. Event symmetry analysis, analytical solutions, and conservation laws of both total and fractional nonlinear models [22–24] have attracted more attention day by day. The space time fractional Burger (sFB) [8–10]

and the time fractional Sharma-Tasso-Olver (tFSTO) [9, 11] models are among the most important fractional models to acquire deep understandings in real nonlinear phenomena in the relevant fields. Both the sFB and tFSTO models are initially converted from the generalized Burger model with some parameter evaluations which have many applications in stochastic problem, water and shock waves, gas dynamics, acoustic science, thermal conduction, etcetera.

Motivated by the importance of the fractional models of sFB and tFSTO and their solutions, present investigation shed the light on the new approach for solving the space time fractional Burger (sFB) and the time fractional Sharma-Tasso-Olver (tFSTO) models by introducing Modified Kudryashov method (MKM). Moreover, we went to derive multishock soliton solutions of the models. Hence, the structure of this paper is as follows: In Section 2, we incorporate definition of conformable fractional derivative and some of its properties. In Section 3, we describe details on the proposed Modified Kudryashov method (MKM) and its applications. In Section 4, we derive new plentiful analytic solutions of the sFBM and the tFSTOM models. Next, we present different types of shapes of the gained wave solutions in 3D and 2D graphics, respectively, in Section 5. Finally, the conclusions of this research are deduced in the last part.

2. Conformable Fractional Derivative and Its Properties

In this section, some important properties of the conformable fractional derivatives according to fractional calculus theory in [3–5] are revisited:

Let us consider a function $\phi : (0,\infty) \longrightarrow \mathfrak{R}$ where the conformable fractional derivative of ϕ with order δ is defined as $\partial^\delta \phi/\partial t^\delta = \lim_{\varepsilon \longrightarrow 0^+} (\phi(t + \varepsilon t^{1-\delta}) - \phi(t)/\varepsilon)$, $t > 0$ and $0 < \delta \leq 1$.

Hence, few key properties of the fractional derivative are given as:

$$\begin{aligned} &\frac{\partial^\delta}{\partial t^\delta}(l\phi + m\psi) = l\frac{\partial^\delta}{\partial t^\delta}(\phi) + m\frac{\partial^\delta}{\partial t^\delta}(\psi), \forall l, m \in \mathfrak{R}, \\ &\frac{\partial^\delta}{\partial t^\delta}\left(t^\beta\right) = \beta t^{\beta-\delta}, \forall \beta \in \mathfrak{R}, \end{aligned} \tag{1}$$

and

$$\begin{aligned} &\frac{\partial^\delta}{\partial t^\delta}(\lambda) = 0, \lambda = \text{const.}, \\ &\frac{\partial^\delta}{\partial t^\delta}(\phi \circ \psi)(t) = t^{1-\delta}\phi'(\psi(t))\psi'(t). \end{aligned} \tag{2}$$

3. The Proposed Modified Kudryashov Method (MKM)

Here with onwards, we will extend the Kudryashov method by using a new suitable integration technique so that our modified method of Kudryashov can further be applied to any nonlinear evolution equations. Let us consider a general form of any nonlinear model as

$$Q\left(U, D_x^\alpha D_t^\beta U, D_x^\alpha D_x^\alpha U, D_x^\alpha U, D_t^\beta U, \cdots \cdots ..\right) = 0, 0 < \alpha, \beta < 1. \tag{3}$$

Note that Q is a polynomial of $U = U(x,t)$ and its various partial fractional derivatives D^α include the nonlinear terms.

Step-01. To convert the nonlinear partial differential Eq. (5) into ordinary differential equation (ODE), we first use the traveling variable,

$$U(x,t) = U(\xi), \xi = \frac{kx^\alpha}{\Gamma(1+\alpha)} - \frac{\omega x^\beta}{\Gamma(1+\beta)}, \tag{4}$$

where k, ω are nonzero constants. Applying the chain rule

$$D_x^\alpha U = \rho_x \frac{\mathrm{d}U}{d\xi} D_x^\alpha \xi, D_t^\beta U = \rho_t \frac{dU}{d\xi} D_t^\beta \xi, \tag{5}$$

where ρ_x, ρ_t are sigma indexes [3] which can be written as $\rho_x, \rho_t = K(\text{const.})$.

Now, by inserting Eq. (4) along with (5) into Eq. (3), we can reach an ordinary differential equation as follows:

$$Q_1\left(U_\xi, U_{\xi\xi\xi}, U_{\xi\xi}, UU_\xi, U_{\xi\xi\xi}, .. \cdots \cdots\right) = 0. \tag{6}$$

Next, we will integrate Eq. (6) as many times as possible while keeping every integral constant to be zero.

Step-2. Assuming the solution of Eq. (6) takes the general form of a polynomial function $F(\xi)$, we can write

$$U(\xi) = \frac{\sum_{i=0}^{N} a_i (F(\xi))^i}{\sum_{j=0}^{M} b_j (F(\xi))^j}, \tag{7}$$

where $a_i, b_j, \omega, k, i = 0, \cdots \cdots, m, j = 0, \cdots \cdots, n$ are constants to be evaluated later. Here, $a_N \neq 0, b_M \neq 0$ whereas N and M are positive integers, which can be found from the principle of balancing technique. Next, we have a condition of $F(\xi)$ that satisfies the general form of the Riccati equation,

$$F'(\xi) = A + BF(\xi) + CF^2(\xi). \tag{8}$$

Step-3. By substituting Eq. (7) into Eq. (6) and using the ODE (8), we can execute a polynomial for $F(\xi)$ by collecting all same order of $F(\xi)$ together. Equating coefficients of $F(\xi)$ yields a set of algebraic systems for $a_i, b_j, \omega, k, i = 0, \cdots \cdots, m, j = 0, \cdots \cdots, n$. Solving the unknowns and setting them into Eq. (7), we can attain the analytic and exact traveling wave solutions of the nonlinear model in Eq. (3).

It is further pointed out that diverse types of solutions are possible for (8):

Case-1: When $B = 0, C = 1$, then (8) has the solution

$$F(\xi) = \begin{cases} -\sqrt{-A}\tanh\left(\sqrt{-A}\xi\right), A < 0 \\ -\sqrt{-A}\coth\left(\sqrt{-A}\xi\right), A < 0 \end{cases}, \quad (9)$$

$$F(\xi) = -\frac{1}{\xi}, A = 0, \quad (10)$$

$$F(\xi) = \begin{cases} \sqrt{A}\tan\left(\sqrt{A}\xi\right), A > 0 \\ -\sqrt{A}\cot\left(\sqrt{A}\xi\right), A > 0 \end{cases}. \quad (11)$$

Case-2: When $A = 0, B = -1, C = 1$, then (8) has the solution

$$F(\xi) = \frac{1}{1 + he^{\xi}}. \quad (12)$$

Case-3: When $C = 0$, then (8) has the solution

$$F(\xi) = \frac{he^{B\xi} - A}{B}. \quad (13)$$

In general, there may have more solutions of (8), but that will be applicable when we can solve any nonlinear models without particular values of the constants A, B, C.

Remark. When we consider the particular values $A = 0$, $B = -1, C = 1$ in the auxiliary equation of the proposed method, we reach to the generalized Kudryashov method [12, 13] and when $b_0 = 1, b_j = 0$ in the trail solution (7) of our method, then we reach to the extended Kudryashov method [14]. Thus, the methods [12–14] are the special cases of this newly proposed MKM.

4. Applications to the Models

In these parts, we present the applications of the MKM for obtaining exact traveling wave solutions to the space fractional Burgers and the time fractional Sharma-Tasso-Olver models. Additionally, we present multishock wave solutions by a different approach of the models.

4.1. The sFBM and tFSTOM Models. The sFBM model given by Eq. (14) is a nonlinear model of diffusive waves which found many applications in fluid dynamics, one-dimensional soundwaves in a viscous medium, gas dynamics, shock waves in a viscous medium, magneto-hydrodynamic waves in a medium with finite electrical conductivity, turbulence, and in plasma dynamics applied to unsaturated flow in field soils [8–10]. This model has the usual form [8–10]:

$$\nu_t + \nu\nu_x - k\nu_{xx} + qD_x^{\delta}\nu = 0, x, t > 0, 0 < \delta \le 1, \nu(0, t) = 0, \nu_x(0, t) = \frac{1}{t} - \frac{\pi^2}{2kt^2}, \quad (14)$$

where k, q are constants and δ is an aspect relating to the order of the fractional derivative.

On the other hand, the tFSTOM model has real-life applications in the fields of relativistic quantum atom dynamics, the relativistic energy evaluation, and the nonlinear electromagnetic phenomena. The tFSTOM model has the usual form [9, 11]:

$$D_t^{\delta}\nu + 3a\nu_x^2 + 3a\nu^2\nu_x + 3a\nu\nu_{xx} + a\nu_{xxx} = 0, t > 0, 0 < \delta < 1, \nu(x, 0) = -\sqrt{2b_0}\tan\left(\frac{\sqrt{2b_0}}{2}x\right), \quad (15)$$

where a, b_0 are constants and δ is an aspect relating to the order of the fractional derivative.

4.2. The Application of the MKM to the sFBM. In this section, we explore a reliable treatment to the sFBM with the help of the MKM.

Primarily, we will use the traveling wave variable, $\nu(x, t) = \nu(\xi), \xi = lx^{\delta}/\Gamma(1 + \delta) - wt$, to renovate Eq. (14) to the following ordinary differential equation:

$$-w\nu' + l\nu\nu' - kl^2\nu'' + ql\nu' = 0. \quad (16)$$

Integrating (16) one time gives us

$$p + (lq - w)\nu + l\nu^2/2 - kl^2\nu' = 0, \quad (17)$$

where p is an integral constant.

Now we compute the balance number of Eq. (17) from the linear terms ν'' and ν^3 gives $n = m + 1$. For $m = 1$, we have $n = 2$. So, the trial solution of Eq. (7) takes the following form,

$$\nu(\xi) = \frac{l_0 + l_1F(\xi) + l_2(F(\xi))^2}{m_0 + m_1F(\xi)}. \quad (18)$$

We now differentiate Eq. (18) with respect to ξ along with Eq. (8), and then inserting ν, ν' intoEq. (17), which gives an equation. Equating the coefficients of $F^l(\xi)$ from the required equation equal to zero yields the following set of constraints:

Set-1:

$$p = \frac{2k^2l^3C\left(Am_1^2 + Bm_0m_1 - Bm_1^2 + Cm_0^2 - 2Cm_0m_1 + Cm_1^2\right)}{m_1^2}, \quad w = l(q + 2Ckl - Bkl - 2Cklm_0/m_1), \quad l_0 = 2Cklm_0(m_1 - m_0)/m_1, l_1 = 2Cklm_1, l_2 = 2Cklm_1. \quad (19)$$

Set-2:

$$p=\frac{\left[2Ck^2l^3m_1(Am_1-Bm_0)^2\left\{(2m_0+m_1)\left(A^2Bm_1^4+A^2Cm_1^4-2AB^2m_0\mathrm{m}_1^3\right)+4BC^2m_0^4(m_0-m_1)+2ABCm_0m_1^2\left(4m_0^2-m_0m_2-1\right)+4AC^2m_0^3m_1^2+2B^2m_0^2m_1\left(Bm_0m_1+Bm_1^2-4Cm_0^2\right)+B^2Cm_0^2m_1^3\right\}\right]}{\left(Am_1^2-Bm_0m_1+2Cm_0^2\right)^4},$$

$$w=\frac{\left\{l\left[kl\left\{ABm_1^2\left(Am_1^2-2Bm_0\right)+2A^2Cm_1^3(m_0+m_1)-2ABCm_0m_1^2(m_0+2m_1)+m_0^2m_1\left(4AC^2+B^3m_1\right)+2B^2Cm_0^2\left(m_1^2-2m_0^2\right)\right\}+q\left\{m_1^2\left(A^2m_1^2+B^2m_0^2\right)-2Am_0m_1^2(Bm_1-2Cm_0)-4Cm_0^2(Bm_1-C)\right\}\right]\right\}}{\left(Am_1^2-Bm_0m_1+2Cm_0^2\right)^2},$$

$$l_0=\frac{2klm_1(Am_1-Bm_0)^2\left(Bm_0m_1+Cm_0m_1-Am_1^2-2Cm_0^2\right)}{\left(Am_1^2-Bm_0m_1+2Cm_0^2\right)^2},$$

$$l_1=\frac{2Cklm_1^3(Am_1-Bm_0)}{\left(Am_1^2-Bm_0m_1+2Cm_0^2\right)^2},$$

$$l_2=\frac{2Cklm_1^2(Bm_0-Am_1)}{Am_1^2-Bm_0m_1+2Cm_0^2}. \tag{20}$$

Set-3:

$$p=\frac{B\left\{8BC^3(kll_2m_0)^2(2A+B)+B^3l_2^3(l_2-4Cklm_0)-32\left(2C^3k^2l^2m_0^2+BCkll_2m_0\right)R\right\}}{128C^6k^2lm_0^4},$$
$$w=\frac{8C^3klqm_0^2-4B^2Ckll_2m_0+B^2l_2^2}{8C^3km_0^2},\ l_0=\pm\frac{R}{m_0klC^3},\ l_1=\frac{Bl_2^2}{4C^2klm_0},\ m_1=\frac{2Cm_0}{B}, \tag{21}$$

where

$$R=-\frac{1}{8B}\left\{4C^3(klm_0)^2\left(4AC-B^2\right)+B^3l_2(2Cklm_0-l_2)\pm2\sqrt{(Cklm_0)^2(4AC-B^2)\left\{4C^4(klm_0)^2(4AC-B^2)+B^3l_2(4Cklm_0-l_2)\right\}}\right\}. \tag{22}$$

Setting the constraints of Set-1 into (18) along with the results of auxiliary equation from Case-1, Case-2, and Case-3 of our method, we attain the following solutions:

Case-1S1: For $B=0, C=1$, the gained solutions are:

$$v_1(x,t)=\frac{2klm_0(m_1-m_0)/m_1-2klm_1\sqrt{-A}\tanh\left(\sqrt{-A}\xi\right)-2Aklm_1\tanh^2\left(\sqrt{-A}\xi\right)}{m_0-m_1\sqrt{-A}\tanh\left(\sqrt{-A}\xi\right)},A<0, \tag{23}$$

$$v_2(x,t)=\frac{2klm_0(m_1-m_0)/m_1-2klm_1\sqrt{-A}\coth\left(\sqrt{-A}\xi\right)-2Aklm_1\coth^2\left(\sqrt{-A}\xi\right)}{m_0-m_1\sqrt{-A}\coth\left(\sqrt{-A}\xi\right)},A<0, \tag{24}$$

$$v_3(x,t)=\frac{\{2klm_0(m_1-m_0)\}\xi^2-2klm_1^2\xi+2klm_1^2}{m_1\left(m_0\xi^2-m_1\xi\right)}, \tag{25}$$

$$v_4(x,t)=\frac{2klm_0(m_1-m_0)/m_1+2klm_1\sqrt{A}\tan\left(\sqrt{A}\xi\right)+2Aklm_1\tan^2\left(\sqrt{A}\xi\right)}{m_0+m_1\sqrt{A}\tan\left(\sqrt{A}\xi\right)},A>0, \tag{26}$$

$$v_5(x,t)=\frac{2klm_0(m_1-m_0)/m_1-2klm_1\sqrt{A}\cot\left(\sqrt{A}\xi\right)+2Aklm_1\cot^2\left(\sqrt{A}\xi\right)}{m_0-m_1\sqrt{A}\cot\left(\sqrt{A}\xi\right)},A>0, \tag{27}$$

where $\xi = lx^{\delta}/\Gamma(1+\delta) - l(q + 2kl - 2klm_0/m_1)\,t$.

Case-2S1: For $A = 0, B = -1, C = 1$, the gained solutions are:

$$v_6(x,t) = \frac{2klm_1 + 2klm_1\left(1 + he^{\xi}\right) + \{2klm_0(m_1 - m_0)/m_1\}\left(1 + he^{\xi}\right)^2}{m_1\left(1 + he^{\xi}\right) + m_0\left(1 + he^{\xi}\right)^2}, \tag{28}$$

where $\xi = lx^{\delta}/\Gamma(1+\delta) - l(q + 2kl + kl - 2klm_0/m_1)t$.

Case-3S1: The third case gives the invalid results as $C = 0$, gives $l_2 = 0$.

Setting the constraints of Set-2 into (18) along with results of auxiliary equation from Case-1, Case-2, and Case-3 of our method, we further attain the following solutions:

Case-1S2: For $B = 0, C = 1$, the gained solutions are:

$$v_7(x,t) = \frac{\left\{2A^2klm_1^3\left(m_0m_1 - Am_1^2 - 2m_0^2\right) - 2A^2klm_1^5\sqrt{-A}\tanh\left(\sqrt{-A}\xi\right) + 2A^2klm_1^3\left(Am_1^2 + 2m_0^2\right)\tanh^2\left(\sqrt{-A}\xi\right)\right\}}{\left(Am_1^2 + 2m_0^2\right)^2\left\{m_0 - m_1\sqrt{-A}\tanh\left(\sqrt{-A}\xi\right)\right\}}, A < 0,$$

$$v_8(x,t) = \frac{\left\{2A^2klm_1^3\left(m_0m_1 - Am_1^2 - 2m_0^2\right) - 2A^2klm_1^5\sqrt{-A}\coth\left(\sqrt{-A}\xi\right) + 2A^2klm_1^3\left(Am_1^2 + 2m_0^2\right)\coth^2\left(\sqrt{-A}\xi\right)\right\}}{\left(Am_1^2 + 2m_0^2\right)^2\left\{m_0 - m_1\sqrt{-A}\coth\left(\sqrt{-A}\xi\right)\right\}}, A < 0,$$

$$v_9(x,t) = \frac{\left\{2A^2klm_1^3\left(m_0m_1 - Am_1^2 - 2m_0^2\right) + 2A^2klm_1^5\sqrt{A}\tan\left(\sqrt{A}\xi\right) - 2A^2klm_1^3\left(Am_1^2 + 2m_0^2\right)\tan^2\left(\sqrt{A}\xi\right)\right\}}{\left(Am_1^2 + 2m_0^2\right)^2\left\{m_0 + m_1\sqrt{A}\tan\left(\sqrt{A}\xi\right)\right\}}, A > 0,$$

$$v_{10}(x,t) = \frac{\left\{2A^2klm_1^3\left(m_0m_1 - Am_1^2 - 2m_0^2\right) - 2A^2klm_1^5\sqrt{A}\cot\left(\sqrt{A}\xi\right) - 2A^2klm_1^3\left(Am_1^2 + 2m_0^2\right)\cot^2\left(\sqrt{A}\xi\right)\right\}}{\left(Am_1^2 + 2m_0^2\right)^2\left\{m_{0_{m_1\sqrt{A}\cot\left(\sqrt{A}\xi\right)}}\right\}}, A > 0, \tag{29}$$

where $\xi = lx^{\delta}/\Gamma(1+\delta) - l\{2A^2klm_1^3(m_0 + m_1) + 4Aklm_0^2m_1 + 4q(A^2m_1^4 + Am_0^2m_1^2 + m_0^4)\}t/(Am_1^2 + 2m_0^2)^2$.

Case-2S2: For $A = 0, B = -1, C = 1$, the gained solutions are:

$$v_{11}(x,t) = \frac{-2klm_0m_1^2\left(m_0m_1 + 2m_0^2\right) + 2klm_0^2m_1^3\left(1 + he^{\xi}\right) - 4klm_1m_0^2\left(1 + he^{\xi}\right)^2}{\left(m_0m_1 + 2m_0^2\right)^2\left\{m_1\left(1 + he^{\xi}\right) + m_0\left(1 + he^{\xi}\right)^2\right\}}, \tag{30}$$

where $\xi = lx^{\delta}/\Gamma(1+\delta) - l\{klm_0^2(4m_0^2 + m_1^2) + qm_0^2(4m_0^2 + 4qm_0m_1 + m_1^2)\}t/(m_0m_1 + 2m_0^2)^2$.

Case-3S2: The third case gives the invalid results as $C = 0$, gives $l_2 = 0$.

Setting the constraints of Set-3 into (18) along with results of auxiliary equation from Case-1, Case-2, and Case-3 of our method, we attain the following solutions:

Case-1S3: For $B = 0, C = 1$, Case-1 and Case-3 give the undefined statements.

Case-2S3: For $A = 0, B = -1, C = 1$, the gained solutions are:

$$v_{12}(x,t) = \frac{4klm_0l_2 - l_2^2\left(1 + he^{\xi}\right) \pm 4R\left(1 + he^{\xi}\right)^2}{4klm_0^2\left(1 + he^{\xi}\right)\left(he^{\xi} - 1\right)}, \tag{31}$$

where $\xi = lx^{\delta}/\Gamma(1+\delta) - (8kqlm_0^2 - 4kll_2m_0 + l_2^2/8km_0^2)t$ and $R = l_2^2/8 - k^2l^2m_0^2 - 1/2kll_2m_0$ or $(l_2^2/8)$.

Case-3S3: The third case gives the invalid results as $C = 0$, gives $l_2 = 0$.

4.3. The Multishock Waves to the Time sFBM. In this section, we now explore a reliable technique to achieve multishock wave of the fractional model. To do so, we consider the simple Burger equation

$$v_t - 2vv_x - v_{xx} = 0. \tag{32}$$

Taking traveling variable $v(x,t) = Y(\xi), \xi = lx - \omega t$, Eq. (32) leads to ODE as follows:

$$Y_{\xi}(x,t) = Y - \frac{1}{l}Y^2. \tag{33}$$

Equation (33) has a multisoliton solution [21].

$$Y = \frac{\sum_{j=1}^{n} l_j e^{l_j x - w_j t}}{1 + \sum_{j=1}^{n} e^{l_j x - w_j t}}. \tag{34}$$

Let us consider the trial solution of Eq. (17) is

$$v = a_0 + a_1 Y. \text{ [as balance number of Burger model is unity]} \tag{35}$$

Keeping arbitrary constant $p = 0$ in Eq. (17), differentiating Eq. (35) together with Eq. (33) into Eq. (17), leads an algebraic system and solving, we reach to multisoliton shock wave solution

$$v = 2k\sum_{j=1}^{n} l_j - \frac{2k\sum_{j=1}^{n}\left(\delta l_j/\Gamma(1+\delta)\right)e^{l_j x^\delta/\Gamma(1+\delta)-w_j t}}{1+\sum_{j=1}^{n} e^{l_j x^\delta/\Gamma(1+\delta)-w_j t}}, \tag{36}$$

where

$$w_j = \sum_{j=1}^{n}\left(kl_j^2 + ql_j\right). \tag{37}$$

4.4. The Application of the MKM to the Time FSTOM. In this section, we now explore a reliable treatment to the time FSTOM with the help of the MKM.

Firstly, we will use the traveling wave variable $v(x,t) = v(\xi), \xi = x - lt^\delta/\Gamma(1+\delta)$, to renovate Eq. (4) to the following ordinary differential equation:

$$-lv' + 3a\left(v'\right)^2 + 3av^2v' + 3avv'' + av''' = 0. \tag{38}$$

Integrating Eq. (38) one time gives us

$$p - lv + 3avv' + av^3 + av'' = 0. \tag{39}$$

Now we compute the balance number of (39) from the linear terms v'' and v^3 gives $n = m + 1$.

For $m = 1$, we have $n = 2$. So, the trial solution of Eq. (7) takes the following form,

$$v(\xi) = \frac{l_0 + l_1F(\xi) + l_2(F(\xi))^2}{m_0 + m_1F(\xi)}. \tag{40}$$

We now differentiate Eq. (40) with respect to ξ along with (10), and then inserting v, v', v'' into Eq. (39), it gives an equation. Equating the coefficients of $F^l(\xi)$ from the required equation equal to zero yields the following findings:

It is very difficult to solve the obtained system of equations in general case even in computational software. Thus, we choose the particular cases (Case-1 and Case-2) to get the results as follows:

Case-1: For $B = 0, C = 1$, the system of equation leads to the solutions:

Set-1: $p = 0, l = -4aA, l_0 = 0, l_2 = l_1, m_0 = -l_1/2, m_1 = -l_1/2$.

Set-2: $p = 0, l = -aA, l_0 = 0, l_2 = l_1, m_0 = -l_1, m_1 = -l_1$.

Setting the constraints of Set-1 into (40) along with the results of auxiliary equation from Case-1 of our method, we attain the following solutions:

Case-1S1: For $B = 0, C = 1$, the gained solutions are:

$$v_1(x,t) = \frac{2\sqrt{-A}\tanh\left\{\sqrt{-A}\left(x+\left(4aAt^\delta/\Gamma(1+\delta)\right)\right)\right\} + 2A\tanh^2\left\{\sqrt{-A}\left(x+\left(4aAt^\delta/\Gamma(1+\delta)\right)\right)\right\}}{1-\sqrt{-A}\tanh\left\{\sqrt{-A}\left(x+\left(4aAt^\delta/\Gamma(1+\delta)\right)\right)\right\}}, A<0, \tag{41}$$

$$v_2(x,t) = \frac{2\sqrt{-A}\coth\left\{\sqrt{-A}\left(x+\left(4aAt^\delta/\Gamma(1+\delta)\right)\right)\right\} + 2A\coth^2\left\{\sqrt{-A}\left(x+\left(4aAt^\delta/\Gamma(1+\delta)\right)\right)\right\}}{1-\sqrt{-A}\coth\left\{\sqrt{-A}\left(x+\left(4aAt^\delta/\Gamma(1+\delta)\right)\right)\right\}}, A<0, \tag{42}$$

$$v_3(x,t) = \frac{-2\sqrt{A}\tan\left\{\sqrt{A}\left(x+\left(4aAt^\delta/\Gamma(1+\delta)\right)\right)\right\} - 2A\tan^2\left\{\sqrt{A}\left(x+\left(4aAt^\delta/\Gamma(1+\delta)\right)\right)\right\}}{1+\sqrt{A}\tan\left\{\sqrt{A}\left(x+\left(4aAt^\delta/\Gamma(1+\delta)\right)\right)\right\}}, A>0, \tag{43}$$

$$v_4(x,t) = \frac{2\sqrt{A}\cot\left\{\sqrt{A}\left(x+\left(4aAt^\delta/\Gamma(1+\delta)\right)\right)\right\} - 2A\cot^2\left\{\sqrt{A}\left(x+\left(4aAt^\delta/\Gamma(1+\delta)\right)\right)\right\}}{1-\sqrt{A}\cot\left\{\sqrt{A}\left(x+\left(4aAt^\delta/\Gamma(1+\delta)\right)\right)\right\}}, A>0. \tag{44}$$

Setting the constraints of Set-2 into (40) along with results of auxiliary equation from Case-1 of our method, we attain to the following solutions:

Case-1S2: For $B = 0, C = 1$, the solutions are:

$$\begin{aligned}
v_5(x,t) &= \frac{\sqrt{-A}\tanh\left\{\sqrt{-A}\left(x+\left(aAt^{\delta}/\Gamma(1+\delta)\right)\right)\right\} + A\tanh^2\left\{\sqrt{-A}\left(x+\left(aAt^{\delta}/\Gamma(1+\delta)\right)\right)\right\}}{1-\sqrt{-A}\tanh\left\{\sqrt{-A}\left(x+\left(aAt^{\delta}/\Gamma(1+\delta)\right)\right)\right\}}, A<0,\\
v_6(x,t) &= \frac{\sqrt{-A}\coth\left\{\sqrt{-A}\left(x+\left(aAt^{\delta}/\Gamma(1+\delta)\right)\right)\right\} + A\coth^2\left\{\sqrt{-A}\left(x+\left(aAt^{\delta}/\Gamma(1+\delta)\right)\right)\right\}}{1-\sqrt{-A}\coth\left\{\sqrt{-A}\left(x+\left(aAt^{\delta}/\Gamma(1+\delta)\right)\right)\right\}}, A<0,\\
v_7(x,t) &= \frac{-\sqrt{A}\tan\left\{\sqrt{A}\left(x+\left(aAt^{\delta}/\Gamma(1+\delta)\right)\right)\right\} - A\tan^2\left\{\sqrt{A}\left(x+\left(aAt^{\delta}/\Gamma(1+\delta)\right)\right)\right\}}{1+\sqrt{A}\tan\left\{\sqrt{A}\left(x+\left(aAt^{\delta}/\Gamma(1+\delta)\right)\right)\right\}}, A>0,\\
v_8(x,t) &= \frac{\sqrt{A}\cot\left\{\sqrt{A}\left(x+\left(aAt^{\delta}/\Gamma(1+\delta)\right)\right)\right\} - A\cot^2\left\{\sqrt{A}\left(x+\left(aAt^{\delta}/\Gamma(1+\delta)\right)\right)\right\}}{1-\sqrt{A}\cot\left\{\sqrt{A}\left(x+\left(aAt^{\delta}/\Gamma(1+\delta)\right)\right)\right\}}, A>0.
\end{aligned} \tag{45}$$

Case-2: For $A = 0, B = -1, C = 1$, the system of equations leads to the solutions:

Set-1:

$$\begin{aligned}
p &= \frac{1}{m_1^2}\frac{\left(2m_0m_1+m_1^2\right)\left\{3a\left(m_0^2-m_0m_1\right)-6am_0^2+12am_0m_1-7am_1^2\right\}}{m_1^2}\\
&\quad + \frac{8am_0\left(m_1-m_0\right)^2}{m_1} + a\left(m_1^2+10m_0m_1-8m_0^2\right),\\
l &= \frac{3a\left(m_0m_1-m_0^2\right)+6am_0^2-12am_0m_1+7am_1^2}{m_1^2}, l_0\\
&= \frac{m_0^2-m_0m_1}{m_1}, l_1 = -m_1, l_2 = -m_1.
\end{aligned} \tag{46}$$

Set-2: $p = 0, l = a, l_0 = 3m_1/2, l_1 = -2m_1, l_2 = -2m_1, m_0 = 3m_1/2$.

Set-3: $p = -12a, l = 13a, l_0 = m_1/2, l_1 = -m_1, l_2 = -m_1, m_0 = -m_1/2$.

Set-4: $p = 0, l = a, l_0 = m_1/2, l_1 = -m_1, l_2 = -m_1, m_0 = m_1/2$.

Set-5:

$$\begin{aligned}
p = 0, l &= -\frac{a\left\{275\left(-3/2\pm\sqrt{17}/2\right)^3+1815\left(-3/2\pm\sqrt{17}/2\right)^2+2412\left(\left(-3/2\pm\sqrt{17}/2\right)^3\right)-2004\right\}}{22\left(-3/2\pm\sqrt{17}/2\right)+78},\\
l_0 &= -\frac{m_1\left\{3\left(-3/2\pm\sqrt{17}/2\right)+11\right\}}{11\left(-3/2\pm\sqrt{17}/2\right)+39}, l_1 = \left(-\frac{3}{2}\pm\frac{\sqrt{17}}{2}\right)m_1, l_2 = -\frac{2m_1}{\left(-3/2\pm\sqrt{17}/2\right)+3}, m_0 = -m_1/2.
\end{aligned} \tag{47}$$

Setting the constraints of Set-1 to Set-5 into (40) along with the results of auxiliary equation from Case-2 yields the solutions:

$$v_9(x,t) = \frac{\left(m_0^2 - m_0 m_1\right)\left(1 + he^{\xi}\right)^2 - m_1^2\left(2 + he^{\xi}\right)}{m_1\left(1 + he^{\xi}\right)\left\{m_0\left(1 + he^{\xi}\right) + m_1\right\}}, \tag{48}$$

$$\xi = x - \frac{\left\{3a\left(m_0 m_1 - m_0^2\right) + 6am_0^2 - 12am_0 m_1 + 7am_1^2\right\}t^{\delta}}{m_1^2\Gamma(1+\delta)}, \tag{49}$$

$$\boldsymbol{v_{10}(x,t)} = \frac{\boldsymbol{-8 - 4h\ \exp\left(x - at^{\delta}/\Gamma(1+\delta)\right) + \left(1 + h\ \exp\left(x - at^{\delta}/\Gamma(1+\delta)\right)\right)^2}}{\boldsymbol{\left(1 + h\ \exp\left(x - at^{\delta}/\Gamma(1+\delta)\right)\right)\left(5 + 3h\ \exp\left(x - at^{\delta}/\Gamma(1+\delta)\right)\right)}}, \tag{50}$$

$$\boldsymbol{v_{11}(x,t)} = \frac{\boldsymbol{-4 - 2h\ \exp\left(x + \left(12at^{\delta}/\Gamma(1+\delta)\right)\right) + \left(1 + h\ \exp\left(x + \left(12at^{\delta}/\Gamma(1+\delta)\right)\right)\right)^2}}{\boldsymbol{\left(1 - h^2\ \exp\left(2x + \left(24at^{\delta}/\Gamma(1+\delta)\right)\right)\right)}}, \tag{51}$$

$$\boldsymbol{v_{12}(x,t)} = \frac{\boldsymbol{-4 - 2h\ \exp\left(x - at^{\delta}/\Gamma(1+\delta)\right) + \left(1 + h\ \exp\left(x - at^{\delta}/\Gamma(1+\delta)\right)\right)^2}}{\boldsymbol{\left(1 + h\ \exp\left(x - at^{\delta}/\Gamma(1+\delta)\right)\right)\left(3 + h\ \exp\left(x - at^{\delta}/\Gamma(1+\delta)\right)\right)}}, \tag{52}$$

$$\boldsymbol{v_{13}(x,t)} = \frac{\boldsymbol{-(6L + 22/11L + 39)\left\{1 + h\ \exp\left(x - lt^{\delta}/\Gamma(1+\delta)\right)\right\}^2 + 2L\left\{1 + h\ \exp\left(x - lt^{\delta}/\Gamma(1+\delta)\right)\right\} - 4/L + 3}}{\boldsymbol{1 - \left\{1 + h\ \exp\left(x - lt^{\delta}/\Gamma(1+\delta)\right)\right\}^2}}, \tag{53}$$

where $l = -a\{275L^3 + 1815L^2 + 2412L - 2004\}/22L + 78$ and $L = -3/2 \pm \sqrt{17}/2$.

4.5. The Multishock Waves to the FSTOM. In this section, we now explore a reliable technique [25] to achieve multishock wave of the fractional FSTOM. To do so, we consider the simple Burger equation (32) and Eq. (33). Then, we consider the wave transformation

$$v(x,t) = v(\xi), \xi = lx - \frac{wt^{\delta}}{\Gamma(1+\delta)}. \tag{54}$$

Using Eq. (54), Eq. (4) leads to

$$-wv' + 3al^2\left(v'\right)^2 + 3alv^2v' + 3al^2vv'' + al^3v''' = 0. \tag{55}$$

Integrating once with putting integral constant as zero, Eq. (55) provides

$$-wv + 3al^2vv' + alv^3 + al^3v'' = 0. \tag{56}$$

Let us consider the trial solution of Eq. (56) is

$$v = a_0 + a_1 Y. [\text{as balance number of the model is unity}] \tag{57}$$

Differentiating Eq. (57) together with Eq. (33) into Eq. (56), leads an algebraic system and solving, we reach to mutlishock wave solution.

$$v = -\sum_{j=1}^{n} l_j + \frac{2\sum_{j=1}^{n} l_j e^{l_j x - wt^{\delta}/\Gamma(1+\delta)}}{1 + \sum_{j=1}^{n} e^{l_j x - wt^{\delta}/\Gamma(1+\delta)}}, \tag{58}$$

where

$$w_j = \sum_{j=1}^{n} al_j^3. \tag{59}$$

5. Numerical Results and Discussions

Numerical illustrations of wave profiles are essential keys for exploration, analysis, and as a tool to communicate the achieved results of the problems coherently. In order to demonstrate the effect of waves in the corresponding application fields, we require definitive knowledge of securing the use of the properties in daily life. Hence, in this section, we physically explain and discuss the features of the solutions of the sFBM and tFSTOM via the MKM in 3D graphics. We discuss the impact of fractionality and parameters on the wave solutions and observe the potential changes of wave properties.

5.1. The Physical Descriptions for the Solutions of the sFBM via the MKM. We present here dynamical properties such as topological kink-dark bell and singular kink, bright bell solitons, and periodic waves of the sFBM. We obtain twelve solutions of the sFBM, among them the solutions $v_1(x,t)$ and $v_7(x,t)$ exhibit solitonic characters while the solutions $v_2(x,t)$ and $v_8(x,t)$ exhibit similar solitonic nature with singularities. Figure 1 represents topological kink-dark bell waves of $v_1(x,t)$. It is signified that the effect of order of

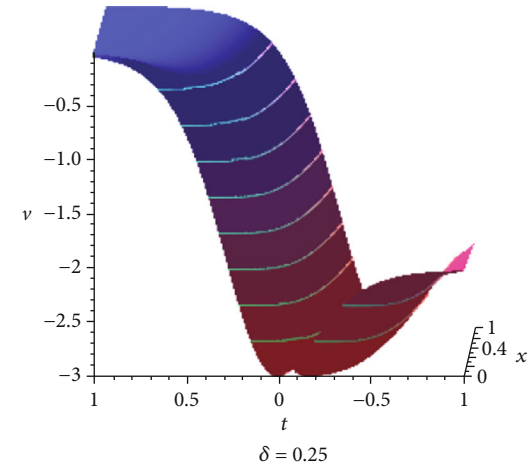

$\delta = 0.25$

(a) $\delta = 0.25$

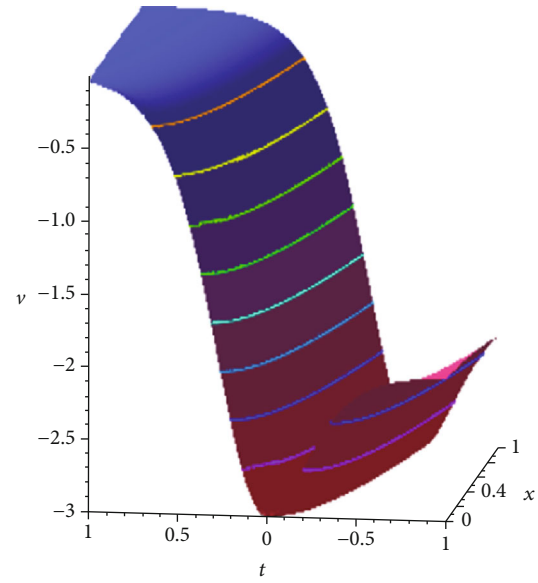

$\delta = 0.5$

(b) $\delta = 0.5$

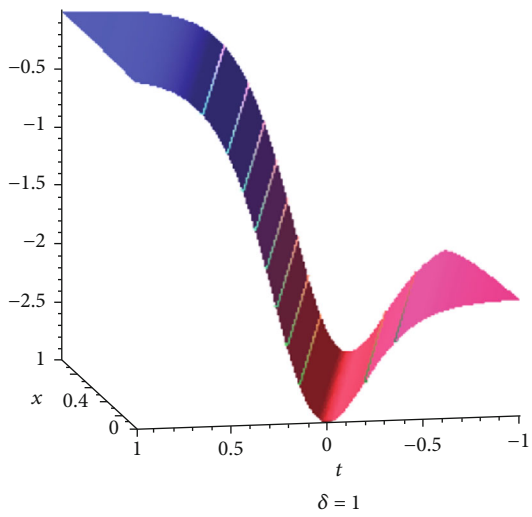

$\delta = 1$

(c) $\delta = 1$

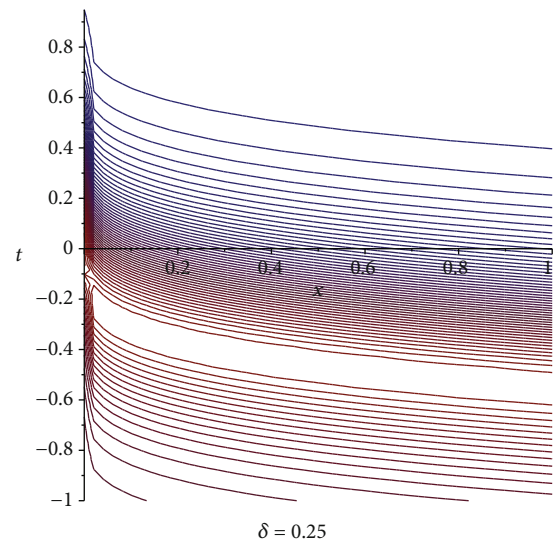

$\delta = 0.25$

(d) $\delta = 0.25$

Figure 1: Continued.

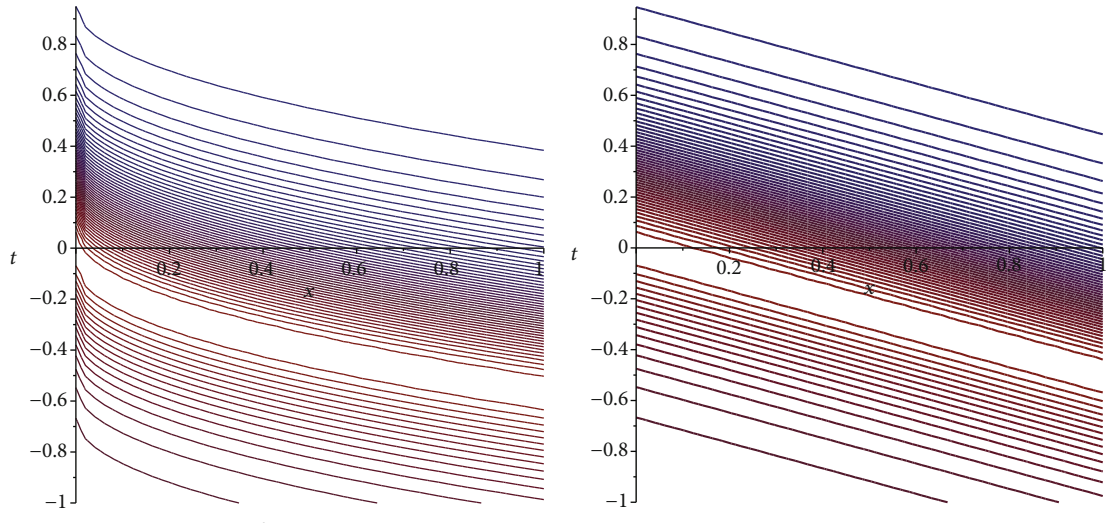

(e) $\delta = 0.25$ (f) $\delta = 1$

FIGURE 1: Topological kink-dark bell wave for $m_1 = 1, m_0 = 2, A = -1, l = 1.5, k = q = 1$ of (23): (a, b) curvy surface for fractional order, (c) straight surface for complete order, (d, e, f) corresponding contour plots of beyond.

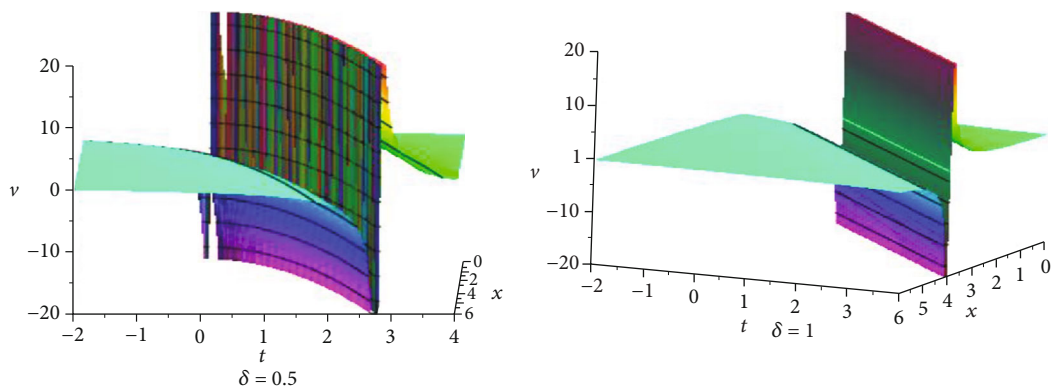

(a) $\delta = 0.5$ (b) $\delta = 1$

FIGURE 2: Topological singular kink wave for $l = k = q = m_0 = m_1 = 1$ of (25): (a) curvy surface for fractional order, (b) straight surface for complete order.

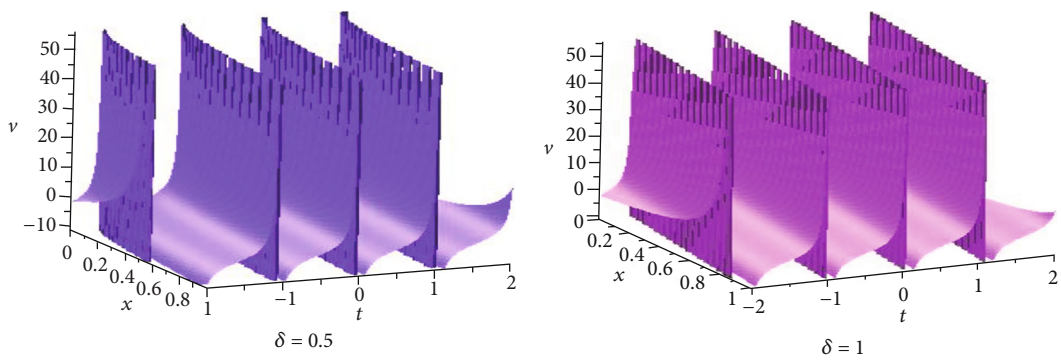

(a) $\delta = 0.5$ (b) $\delta = 1$

FIGURE 3: Periodic wave solution for $m_1 = 1, m_0 = 2, A = 1, l = 1.5, k = q = 1$ of (26): (a) curvy surface for fractional order, (b) straight surface for complete order.

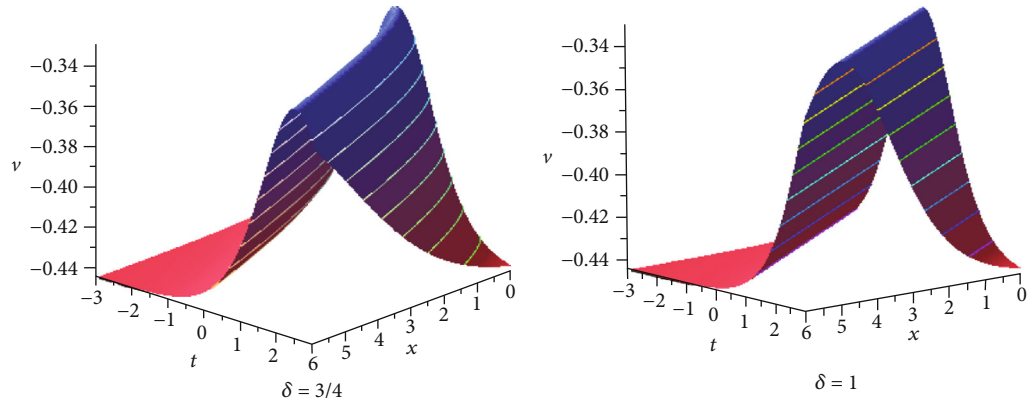

(a) $\delta = 3/4$ (b) $\delta = 1$

FIGURE 4: Bright bell wave for $l = k = q = h = m_0 = m_1 = 1$ of (30): (a) curvy surface for fractional order, (b) straight surface for complete order.

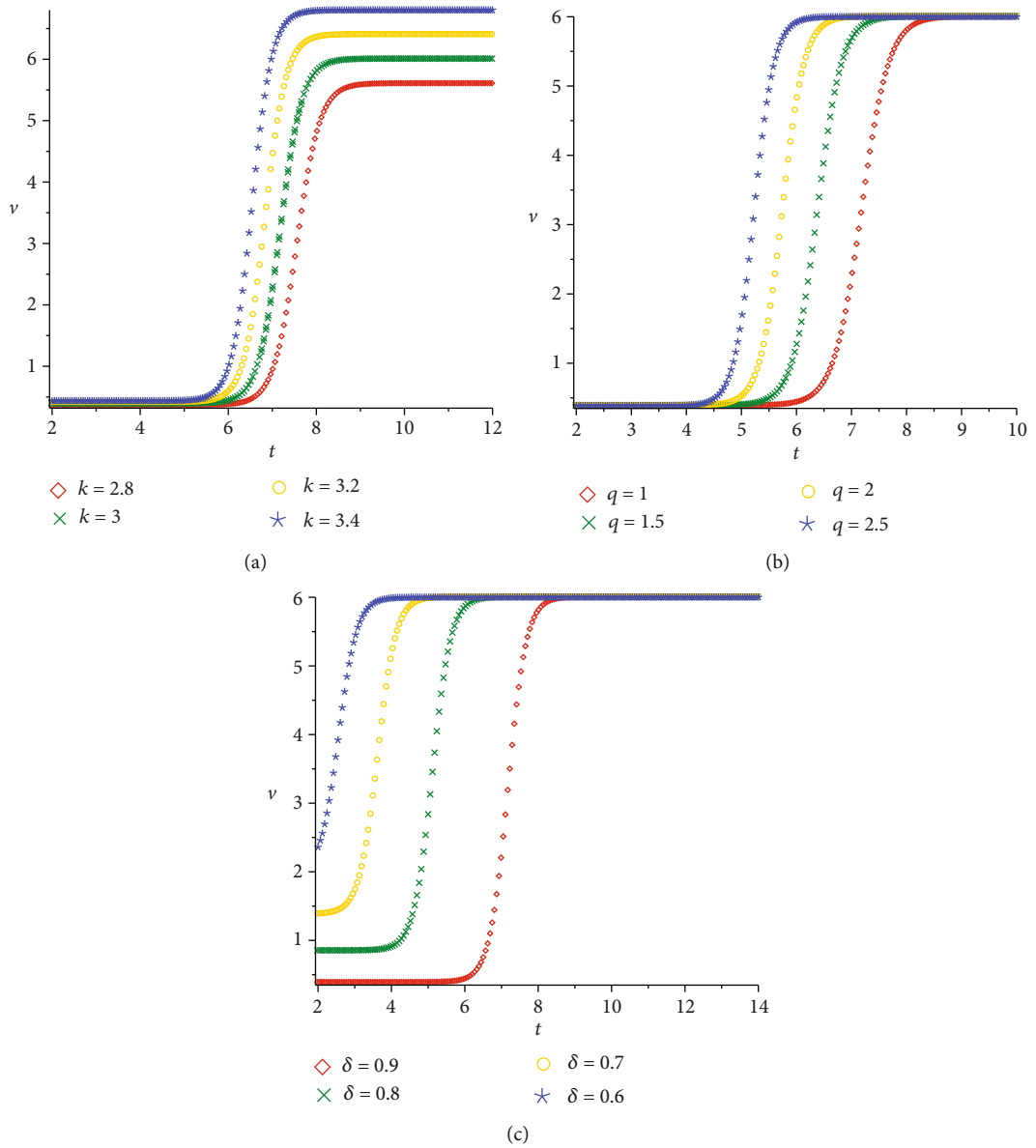

(a) (b) (c)

FIGURE 5: Single shock wave for $l_1 = 1$: (a) $q = 1, \delta = 0.9$, (b) $k = 3, \delta = 0.9, K = 3, q = 1$, and (c) $q = 1, k = 3$ at $x = 40$.

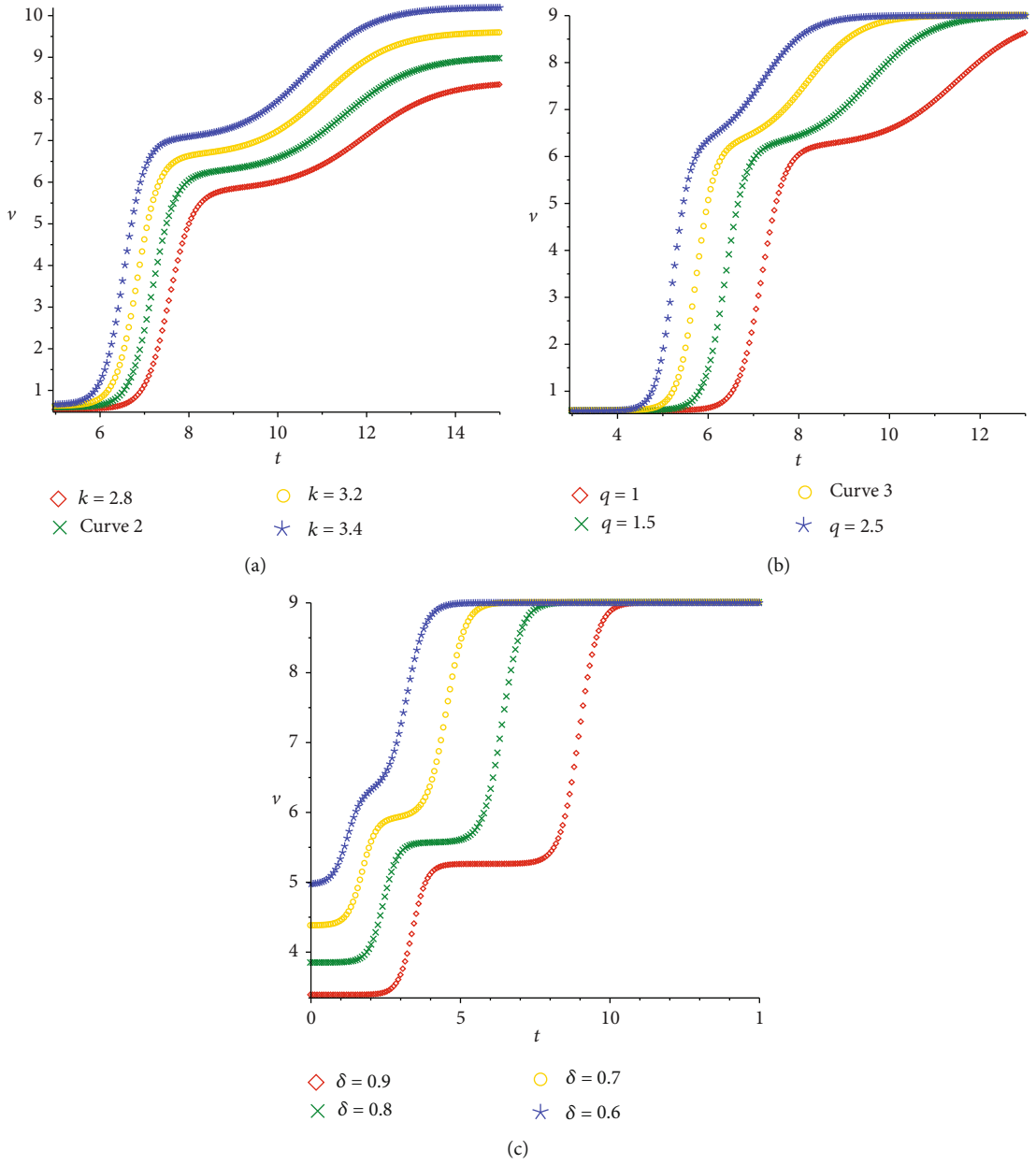

Figure 6: Two shock waves for $l_1 = 1, l_2 = 0.5$: (a) $q = 1, \delta = 0.9$, (b) $k = 3, \delta = 0.9K = 3$, $q = 1$, and (c) $q = 1, k = 3$ at $x = 40$.

differential fractionality is observed on the wave surface which gives the real situation as really most of the natural waves proceed in a curvy pattern. In Figure 1, one can observe that the wave surface is curvier for the lower fractional order (see Figure 1(a) and corresponding contour plot (d)), and curvy pattern gradually reduces to straight line surface as the order of fractionality increases (see Figure 1(b) and corresponding contour plot (e)), and ultimately being straight surface for complete order of the derivative, i.e., $\delta = 1$ (see Figure 1(c) and corresponding contour plot (f)). The solution $\nu_3(x,t)$ comes from the rational solutions as a topological singular kink soliton (see Figure 2). However, the solutions $\nu_4(x,t)$ and $\nu_9(x,t)$ are periodic waves while the solutions $\nu_5(x,t)$ and $\nu_{10}(x,t)$ are similar periodic waves with singularities. Figure 3 represents periodic waves of $\nu_4(x,t)$. Besides, the solutions $\nu_6(x,t), \nu_{11}(x,t)$, and $\nu_{12}(x,t)$ come in terms of exponential functions that exhibit bright bell solitary waves as depicted in Figure 4 of $\nu_{11}(x,t)$. The impact of fractionality is similarly observed in all wave solutions like explanation of Figure 1.

5.2. The Physical Descriptions for the Multishock Wave Solutions of the sFBM. Shock waves and its multistages jumping process (multitimes shocks) are very important in the fields of shock waves in a viscous medium, magnetohydrodynamic waves in a medium with finite electrical conductivity, turbulence, and in plasma dynamics. We present here overtaking collision of multishock waves to the sFBM

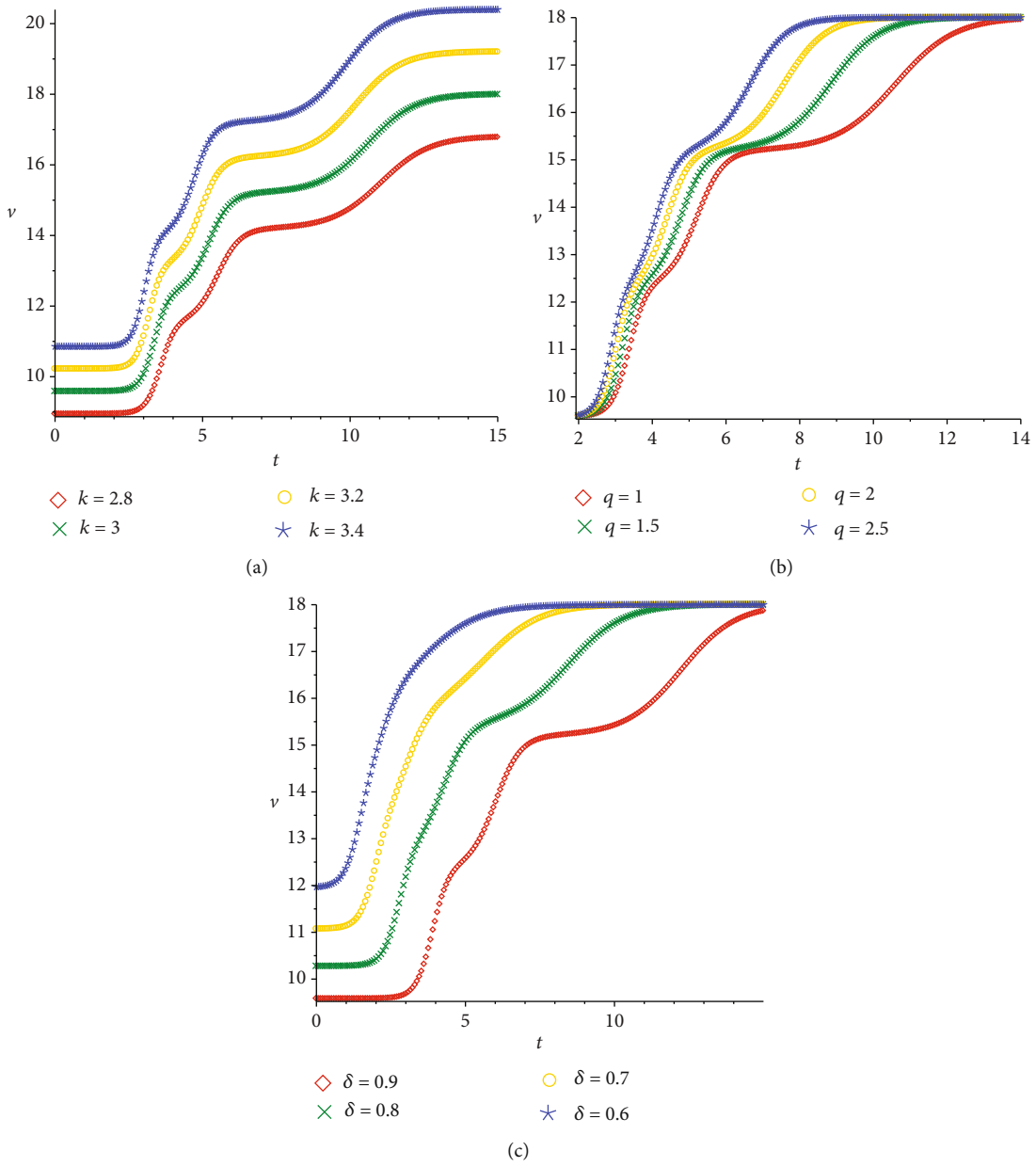

FIGURE 7: Three shock waves for $l_1 = 1, l_2 = 0.5, l_3 = 1.5$: (a) $q = 1, \delta = 0.9$, (b) $k = 3, \delta = 0.9, K = 3, q = 1$, and (c) $q = 1, k = 3$ at $x = 40$.

and its different scattering way, distances from each other, amplitudes, and height of each shock are showed for different changes of parameter a in Figures 5–7. The effect of dispersive parameters k, the coefficient of fractional derivative q , and fractional order on overtaking collisions of multishocks are illustrated graphically.

5.3. The Physical Descriptions for the Solutions of the tFSTOM via the MKM. We present here dynamical properties such as topological kink and singular kink, bright and bark bell solitons, periodic waves, and peakon soliton of the tFSTOM. We obtain thirteen solutions of the tFSTOM, and among them, the solutions $\nu_1(x,t), \nu_5(x,t)$ exhibit solitonic character while $\nu_2(x,t), \nu_6(x,t)$ represent similar solitonic nature with singularities. Figure 8 represents topological kink waves specified by $\nu_1(x,t)$. It is signified that the effect of order of differential fractionality is observed on the wave surface which gives the real situation as really most of the natural waves proceed in a curvy pattern. In Figure 8, one can observe that the wave surface is curvy for the lower fractional order (see Figure 8(a) and corresponding contour plot (d)) and curvy pattern gradually reduces to straight line surface as the order of fractionality increases (see Figure 8(b) and corresponding contour plot (e)), and ultimately being straight surface for complete order of the derivative, i.e., $\delta = 1$ (see Figure 8(c) and corresponding contour plot (f)). The solutions $\nu_3(x,t)$ and $\nu_7(x,t)$ are periodic waves while the solutions $\nu_4(x,t), \nu_8(x,t)$ represent similar

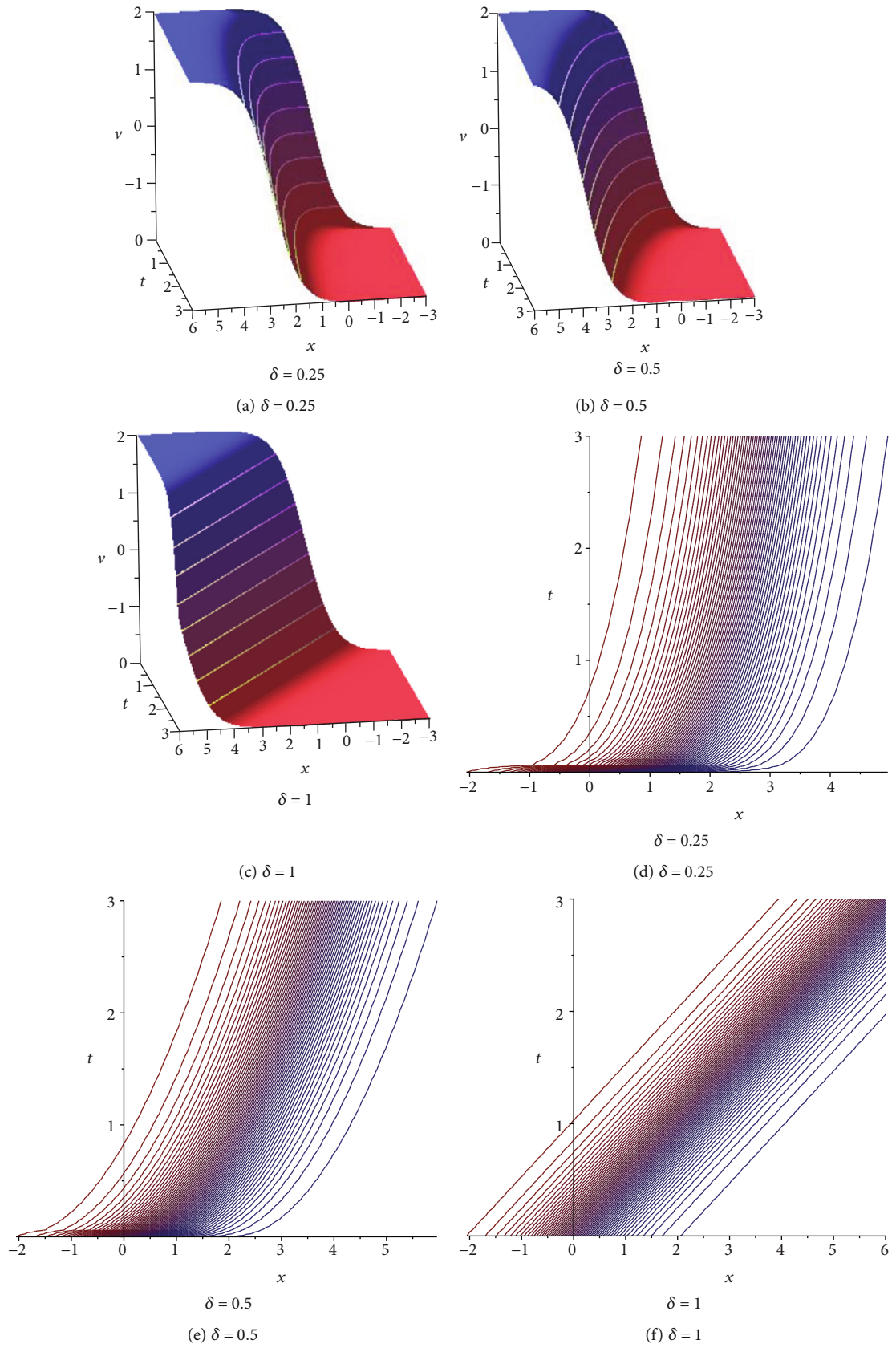

(a) $\delta = 0.25$ (b) $\delta = 0.5$

(c) $\delta = 1$ (d) $\delta = 0.25$

(e) $\delta = 0.5$ (f) $\delta = 1$

FIGURE 8: Topological kink wave for $A = -1$, $a = 0.5$ of (41): (a, b) curvy surface for fractional order, (c) straight surface for complete order, and (d, e, f) corresponding contour plots of (a, b, c).

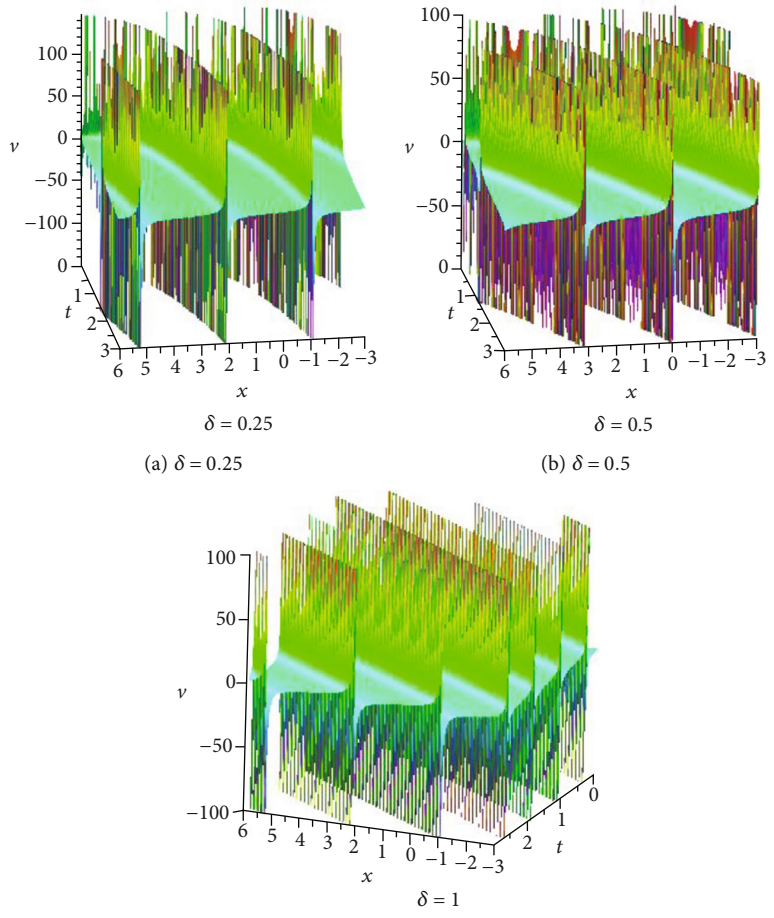

(a) $\delta = 0.25$ (b) $\delta = 0.5$

(c) $\delta = 1$

FIGURE 9: Periodic wave solution for $A = a = 1$ of (43): (a) for $\delta = 0.25$, (b) for $\delta = 0.5$, (c) for $\delta = 1$: (a, b) curvy surface for fractional order, (c) straight surface for complete order.

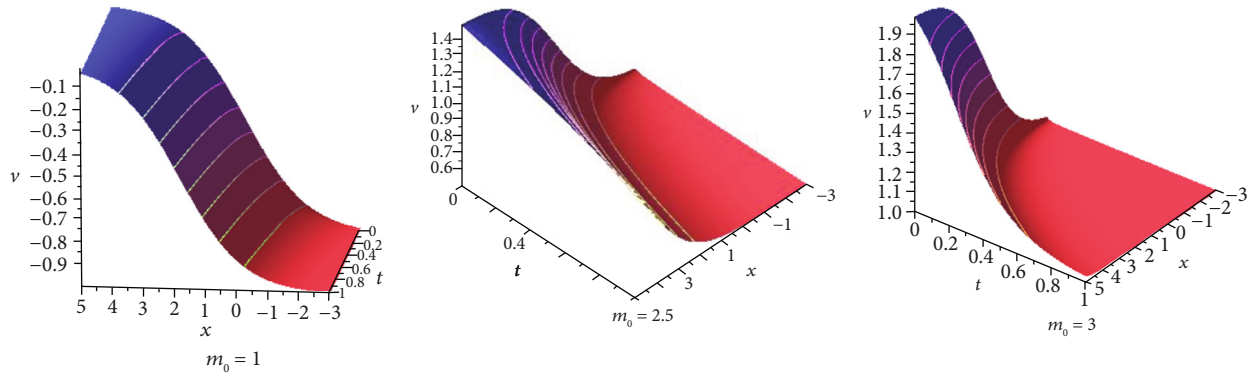

(a) $m_0 = 1$ (b) $m_0 = 2.5$ (c) $m_0 = 3$

FIGURE 10: Kink wave for $A = a = m_1 = 1, \delta = 0.5$ of (48): (a) $m_0 = 1$, (b) $m_0 = 2.5$, (c) $m_0 = 3$: (a, b) curvy surface for fractional order, (c) straight surface for complete order and deform into a single peakon wave.

periodic waves with singularities. Figure 9 represents periodic waves of $v_3(x, t)$. The other solutions of $v_9(x, t), v_{10}(x, t), v_{11}(x, t), v_{12}(x, t)$, and $v_{13}(x, t)$ come in an exponential fashion and represent different solitonic characters for dissimilar values of the existing parameters. Figures 10–12, demonstrate topological kink, singular kink, and dark bell wave solutions by $v_9(x, t)$, $v_{11}(x, t)$, and $v_{13}(x, t)$, respectively. The nature of the solution $v_{10}(x, t), v_{12}(x, t)$ is similar

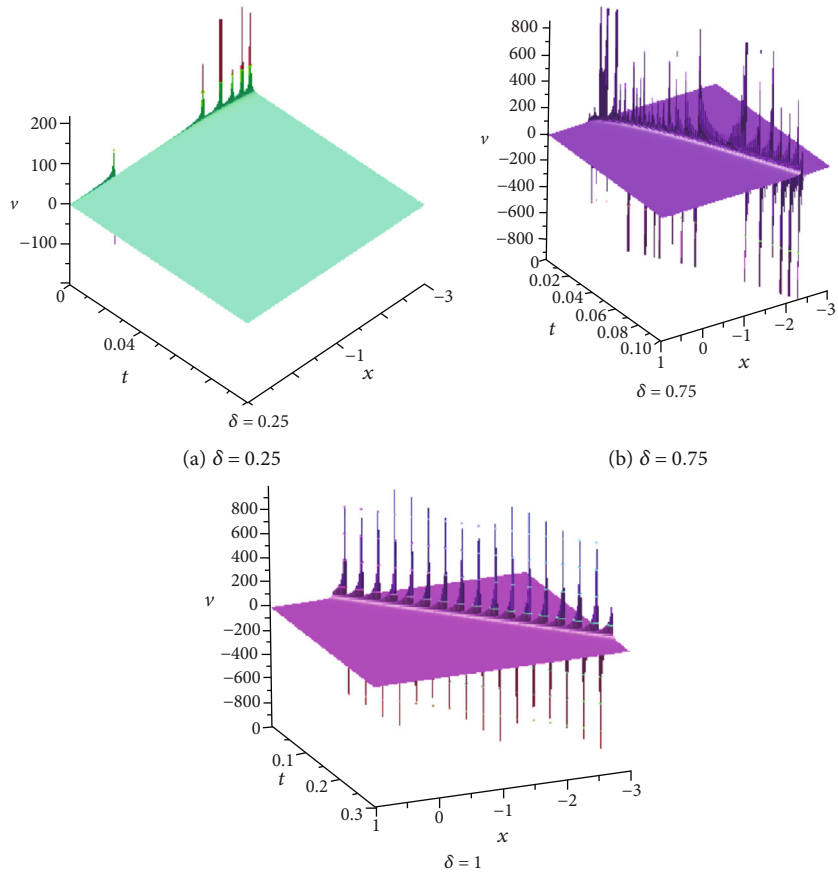

(a) $\delta = 0.25$ (b) $\delta = 0.75$

(c) $\delta = 1$

FIGURE 11: Multipeakon soliton for $a = h = 1$ of (51): (a) multipeakon soliton, (b) singular kink with curvy surface for fractional order, (c) singular kink with multipeakon straight surface for complete order of fractionality.

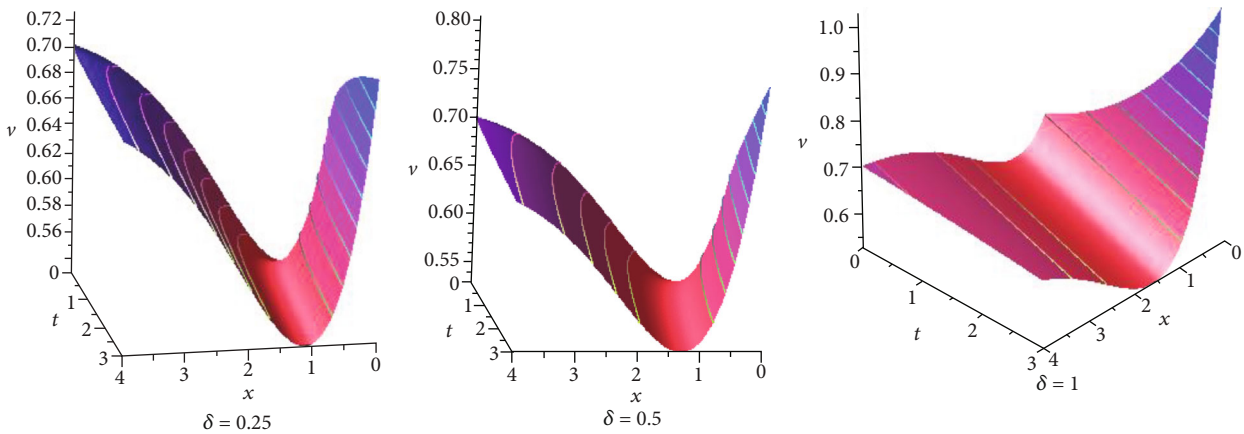

(a) $\delta = 0.25$ (b) $\delta = 0.5$ (c) $\delta = 1$

FIGURE 12: Dark bell wave for $a = h = 1$ of (53): (a, b) curvy surface for fractional order, (c) straight surface for complete order of fractionality.

to the result $v_9(x, t)$ and the nature of the solution deformed into a single peak wave when the fractionality tend to unity (see Figures 10(b) and 10(c)). Besides this, Figure 11 specified by $v_{11}(x, t)$ exhibits multipeakon soliton only for lower fractionality $\delta \longrightarrow 0\,(<0.25)$ (see Figure 11(a)), but it reduces to singular kink wave with multipeak as increases of the fractionality $\delta \longrightarrow 1\,; \delta \in (0, 1)$ (see Figures 11(b) and 11(c)). Figure 12 represents dark bell wave for the

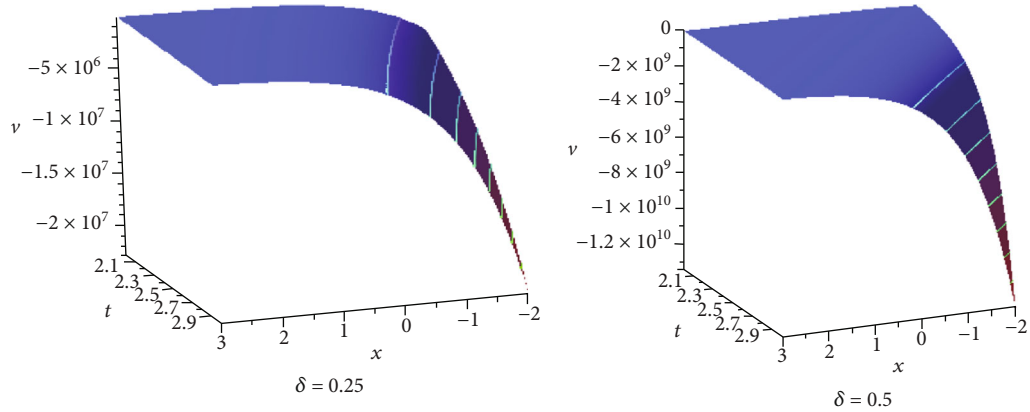

(a) $\delta = 0.25$ (b) $\delta = 0.5$

FIGURE 13: Peakon wave for $a = h = 1$ of (53): $L = -3/2 - \sqrt{17}/2$: (a) curvy surface for fractional order, (b) comparatively straight surface for fractionality $\delta = 0.5$.

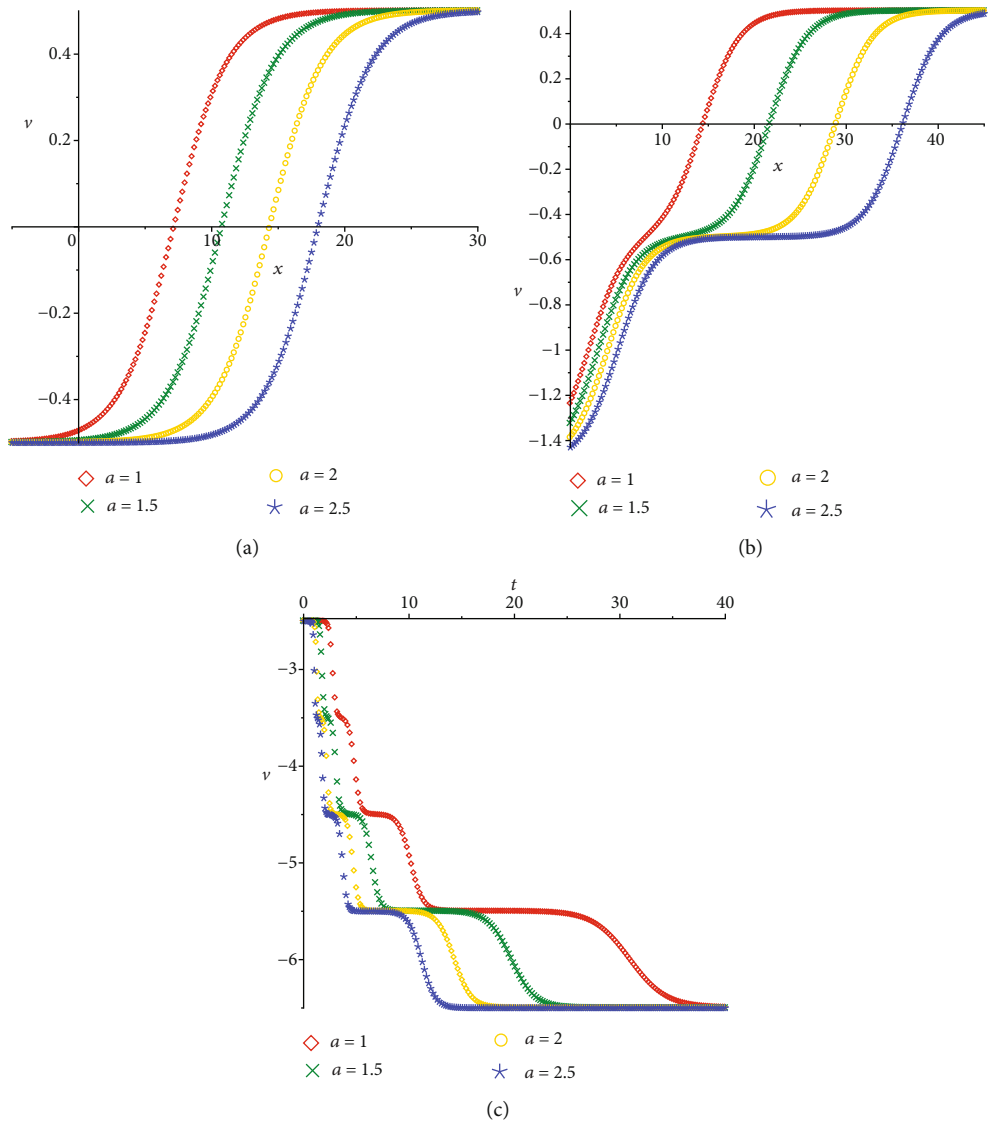

FIGURE 14: (a) Single shock wave for $\delta = 0.9, l_1 = 0.5$ at $t = 40$. (b) Two shock waves for $\delta = 0.9, l_1 = 0.5, l_2 = 1$ at $t = 10$. (c) Five shock waves for $\delta = 0.9, l_1 = 0.5, l_2 = 1, l_3 = 1.5, l_4 = 2, l_5 = 2.5$ at $x = 40$.

parametric value $L = -3/2 + \sqrt{17}/2$, but it is just being a single peak wave depicted by Figure 13 for $L = -3/2 - \sqrt{17}/2$. It is observed for Figure 13 that at the time of interactions or nearer, the waves' height decreases exponentially with utmost deeper peak. The impact of fractionality is similarly observed in all wave solutions like explanation of Figure 8.

5.4. The Physical Descriptions for the Multishock Wave Solutions of the tFSTOM. We present here overtaking collision of multishock waves to the tFSTOM and its different scattering way, amplitudes, and height of each shock are showed for different changes of parameter a in Figure 14. From the view, one interested researcher and engineer might realize the effect of parameters, which parameter, and how the value can proceed quickly to overtake the other waves. Through the images, we can effectively analyze the effect of fractional power and parameters on the wave solutions, and observe the potential changes of characteristics of waves.

6. Conclusions

We have successfully achieved the solitary wave solutions of a class of the conformable sFB and the tFSTO models via the proposed resourceful integral MKM. Periodic, topological kink, singular kink, peakon soliton, and periodic wave soliton solutions are derived by the straight forward approach. The retrieved explicit solutions are presented in a more general form of the fractional differential models. The impact of fractionality on the wave shape and its deformation is analyzed and discussed graphically. Beside this, we achieved multishock wave solutions to the both fractional models and showed the parametric effect on the changes of shock waves. To visualize the real properties of the solutions, the graphical elucidation in 3D and 2D profiles of the gained solutions are presented for suitable parametric selection. Moreover, the generalized Kudryashov [12, 13] and the extended Kudryashov methods [14] are the special cases of this proposed MKM. From our computational effort and achievement, we emphasize that the proposed scheme is very simple, highly effective, and a powerful mathematical tool to extract exact solitary wave solutions of both differential and fractional differential models. The achieved solutions are realistic and appropriate to use and they penetrate the fission and fusion occurrences in solitons, fluid dynamics, sound waves in a viscous medium, gas dynamics, and plasma dynamics.

Data Availability

No data were used to support this study.

Conflicts of Interest

The authors declare that they have no conflicts of interest.

References

[1] J. H. He, S. K. Elegan, and Z. B. Li, "Geometrical explanation of the fractional complex transform and derivative chain rule for fractional calculus," *Physics Letters A*, vol. 376, no. 4, pp. 257–259, 2012.

[2] K. S. Al-Ghafri, "Soliton behaviours for the conformable space–time fractional complex Ginzburg–Landau equation in optical fibers," *Symmetry*, vol. 12, no. 2, p. 219, 2020.

[3] M. Yavuz, N. Ozdemir, and H. M. Baskonus, "Solutions of partial differential equations using the fractional operator involving Mittag-Leffler kernel," *The European Physical Journal Plus*, vol. 133, no. 6, p. 215, 2018.

[4] A. Esen, T. A. Sulaiman, H. Bulut, and H. M. Baskonus, "Optical solitons to the space-time fractional (1+1)-dimensional coupled nonlinear Schrodinger equation," *Optik*, vol. 167, pp. 150–156, 2018.

[5] T. A. Sulaiman, H. Bulut, and H. M. Baskonus, "Optical solitons to the fractional perturbed NLSE in nano-fibers," *Discrete and Continuous Dynamical Systems - Series S*, vol. 13, no. 3, pp. 925–936, 2020.

[6] X. Wang, J. Wei, and X. Geng, "Rational solutions for a (3+1)-dimensional nonlinear evolution equation," *Communications in Nonlinear Science and Numerical Simulation*, vol. 83, article 105116, 2020.

[7] J. Zhang, Z. Wei, L. Yong, and Y. Xiao, "Analytical solution for the time fractional BBM-Burger equation by using modified residual power series method," *Complexity*, vol. 2018, Article ID 2891373, 11 pages, 2018.

[8] M. I. Syam, D. A. Obayda, W. Alshamsi, N. Al-Wahashi, and M. Alshehhi, "Generalized solutions of the fractional Burger's equation," *Results in Physics*, vol. 15, article 102525, 2019.

[9] Ö. Güner and A. C. Cevikel, "A procedure to construct exact solutions of nonlinear fractional differential equations," *The Scientific World Journal*, vol. 2014, Article ID 489495, 10 pages, 2014.

[10] S. Momani, "Non-perturbative analytical solutions of the space- and time-fractional Burgers equations," *Chaos, Solitons & Fractals*, vol. 28, no. 4, pp. 930–937, 2006.

[11] L. N. Song, Q. Wang, and H. Q. Zhang, "Rational approximation solution of the fractional Sharma-Tasso-Olever equation," *Journal of Computational and Applied Mathematics*, vol. 224, no. 1, pp. 210–218, 2009.

[12] M. S. Ullah, H. O. Roshid, M. Z. Ali, and Z. Rahman, "Novel exact solitary wave solutions for the time fractional generalized Hirota–Satsuma coupled KdV model through the generalized Kudryshov method," *Contemporary Mathematics*, vol. 1, no. 1, pp. 25–33, 2019.

[13] M. R. Islam and H. O. Roshid, "Application of generalized Kudryashov method to the Burger equation," *International Journal of Mathematics Trends and Technology*, vol. 38, no. 2, pp. 111–113, 2016.

[14] E. Yasar, Y. Yıldırım, and A. R. Adem, "Perturbed optical solitons with spatio-temporal dispersion in (2 + 1)-dimensions by extended Kudryashov method," *Optik*, vol. 158, pp. 1–14, 2018.

[15] H. O. Roshid, N. Rahman, and M. A. Akbar, "Traveling waves solutions of nonlinear Klein Gordon equation by extended (G'/G)-expansion method," *Annals of Pure and Applied Mathematics*, vol. 3, pp. 10–16, 2013.

[16] H. M. Baskonus, H. Bulut, and A. Atangana, "On the complex and hyperbolic structures of the longitudinal wave equation in a magneto-electro-elastic circular rod," *Smart Materials and Structures*, vol. 25, no. 3, article 035022, 2016.

[17] M. Onorato, S. Residori, U. Bortolozzo, A. Montina, and F. T. Arecchi, "Rogue waves and their generating mechanisms in different physical contexts," *Physics Reports*, vol. 528, no. 2, pp. 47–89, 2013.

[18] H. O. Roshid and W. X. Ma, "Dynamics of mixed lump-solitary waves of an extended (2 + 1)-dimensional shallow water wave model," *Physics Letters A*, vol. 382, no. 45, pp. 3262–3268, 2018.

[19] M. B. Hossen, H. O. Roshid, and M. Z. Ali, "Characteristics of the solitary waves and rogue waves with interaction phenomena in a (2 + 1)-dimensional Breaking Soliton equation," *Physics Letters A*, vol. 382, no. 19, pp. 1268–1274, 2018.

[20] C. Kharif, E. Pelinovsky, and A. Slunyaev, *Rogue Wave in the Ocean*, Springer, 2009.

[21] G. Wang and A. M. Wazwaz, "On the modified Gardner type equation and its time fractional form," *Chaos, Solitons & Fractals*, vol. 155, article 111694, 2022.

[22] G. Wang, "Symmetry analysis, analytical solutions and conservation laws of a generalized KdV-Burgers-Kuramoto equation and its fractional version," *Fractals*, vol. 29, no. 4, article 2150101, 2021.

[23] G. Wang, "A new (3 + 1)-dimensional Schrödinger equation: derivation, soliton solutions and conservation laws," *Nonlinear Dynamics*, vol. 104, no. 2, pp. 1595–1602, 2021.

[24] G. Wang, "A novel (3+1)-dimensional sine-Gorden and a sinh-Gorden equation: derivation, symmetries and conservation laws," *Applied Mathematics Letters*, vol. 113, article 106768, 2021.

[25] C. K. Kuo and S. Y. Lee, "Novel methods for finding general forms of new multi-soliton solutions to (1+1)-dimensional KdV equation and (2+1)-dimensional Kadomtsev–Petviashvili (KP) equation," *Waves in Random and Complex Media*, vol. 29, no. 3, pp. 569–579, 2019.